AIP | Journal of Applied Physics

Electrical characterization of ZnO ceramics by scanning tunneling spectroscopy and beam-induced current in the scanning tunneling microscope

C. Díaz-Guerra and J. Piqueras

Citation: J. Appl. Phys. **86**, 1874 (1999); doi: 10.1063/1.370982
View online: http://dx.doi.org/10.1063/1.370982
View Table of Contents: http://jap.aip.org/resource/1/JAPIAU/v86/i4
Published by the AIP Publishing LLC.

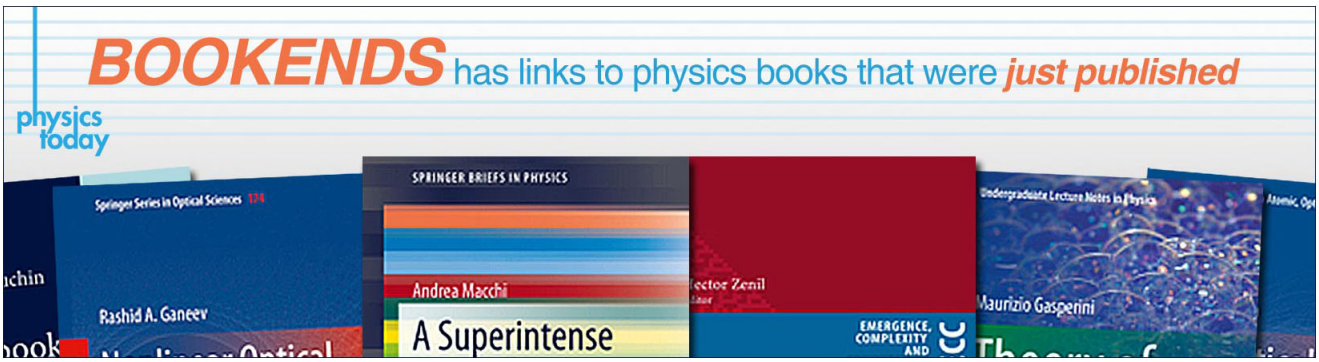

Electrical characterization of ZnO ceramics by scanning tunneling spectroscopy and beam-induced current in the scanning tunneling microscope

C. Díaz-Guerra and J. Piqueras[a)]
Departamento de Física de Materiales, Facultad de Físicas, Universidad Complutense, E-28040 Madrid, Spain

(Received 25 January 1999; accepted for publication 5 May 1999)

A correlative study of the electrically active grain boundary structure of ZnO polycrystals has been carried out using a scanning electron microscope/scanning tunneling microscope (SEM/STM) combined instrument. Current imaging tunneling spectroscopy (CITS) measurements reveal reduced surface band gaps, as compared with grain interiors, at the charged boundaries imaged by SEM-based remote electron beam induced current (REBIC). ZnO grain boundaries were also imaged in the STM-REBIC mode with a resolution of up to 20 nm. The contrast differences observed in the SEM-REBIC and STM-REBIC images are discussed in terms of the different experimental conditions used in both techniques. © *1999 American Institute of Physics.* [S0021-8979(99)01316-X]

I. INTRODUCTION

Some of the main electrical properties of conducting ceramics are related to the presence of space charges, and the associated built-in fields, at the grain boundaries. In particular, the effect of grain boundaries on the ZnO varistor nonlinear electrical characteristic has been related to intrinsic properties at the boundaries, as the oxygen vacancy distribution.[1] An intrinsic layer is formed at the boundary resulting in an *n-i-n* barrier structure. The space charge structures of these barriers have often been investigated by current–voltage, current–temperature, or capacitance–voltage, but spatially resolving methods have been found to provide a complementary and detailed information on the grain boundary barrier including local variations of the electronic properties along the boundary. One of the techniques with spatial resolution which has been used to study electrical barriers in ZnO and other ceramic materials and high-resistivity polycrystalline semiconductors is remote electron beam induced current (REBIC) in the scanning electron microscope (SEM),[2–5] whose resolution is normally of the order of a micron or a fraction of a micron.

Scanning tunneling microscopy (STM) and tunneling spectroscopy (STS) have been extensively used to investigate electronic properties of semiconductors, and some of the STM-based techniques used are analogous to the well-established SEM-based techniques applied in the characterization of the mentioned materials. This is the case of scanning tunneling luminescence (see Ref. 6 for a review), which is similar to cathodoluminescence in the SEM but enables resolution of the order of nanometers. The use of the STM-REBIC or the EBIC techniques has been, contrary to tunneling luminescence, only occasionally reported as in the case of $CuInSe_2$ (Ref. 7) or Si (Ref. 8). In the present work, a combined SEM-STM instrument is used to investigate the electronic behavior of grain boundaries in sintered ZnO. In particular, STM-REBIC and current imaging tunneling spectroscopy (CITS) measurements were performed in specific areas investigated by SEM techniques.

II. EXPERIMENT

The material characterized was undoped ceramic ZnO. The microscope used was a combined SEM-STM, based on a Leica 440 SEM operating under a vacuum of 1×10^{-6} Torr. The small size of the STM enabled it to be mounted on a SEM specimen holder. The main features of the system are similar to the one previously described in Ref. 9.

SEM measurements were performed in secondary electron (SE) and in REBIC modes. For REBIC measurements ohmic contacts, separated about 2 mm on the sample surface, were provided by silver paste and gold wires, and the signal was measured at room temperature with a Matelect ISM-5 system.

For STM measurements, electrochemically etched or mechanically sharpened Pt-Ir wires were used as probe tips. The STM was used in the conventional constant-current mode, in the current-imaging tunneling spectroscopy (CITS) mode, and in the STM-REBIC mode. CITS is one of the spectroscopic modes of STM (Ref. 10) developed by Hamers *et al.*,[11] which provides real space imaging of surface electronic states by recording $I-V$ curves at fixed tip-sample separation at every pixel within an image. In addition to the $I-V$ curves, current images can be formed by plotting the measured current at any voltage. For CITS measurements, the topographic height was recorded at a point of a 128×128 pixel grid, the feedback loop was interrupted for 2 ms and the voltage was digitally ramped from the tunnel voltage to a set of 44 predetermined values while the current was sampled. The tip was then moved to the next point and the process repeated. This provides a set of 44 tunneling current

a)Electronic mail: piqueras@eucmax.sim.ucm.es

FIG. 1. SEM-REBIC image of a ZnO ceramic revealing electrically active grain boundaries in the sample.

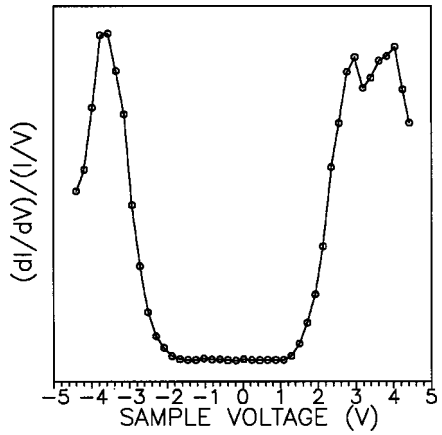

FIG. 2. Normalized differential conductance spectra from a flat surface far from grain boundaries.

files at different voltages, which enables us to plot $I-V$ curves at different points of the image. The tunneling current depends on both tip-sample separation and applied bias voltage. Most of this dependence can be removed[12] by plotting the ratio of differential to total conductance, $(dI/dV)/(I/V)$, which provides a rather direct measure of the surface density of states.[13,14] For this reason, $(dI/dV)/(I/V)$ curves are used here to represent the $I-V$ data. Possible surface contamination due to the SEM electron beam was minimized using beam currents lower than 50 pA and by reducing the observation time necessary to position the STM tip on the grain boundaries.

The contact arrangement for STM-REBIC was similar to that described in Ref. 7, which is the tunnel equivalent of the SEM-REBIC configuration. The two ohmic contacts, separated up to 0.5 mm, were provided by silver paste and gold wires. The tunnel tip was located above the region between the contacts and voltages of up to 6 V were applied.

III. RESULTS AND DISCUSSION

The contrast in the SEM-REBIC images is mainly related to the grain boundaries (Fig. 1). This observation shows the presence of electrically active grain boundaries in our samples and enables us, by using the capabilities of our SEM-STM system, to perform a STM study of regions with different electrical activities. Grain boundaries of ZnO ceramics have been previously imaged by REBIC and different contrasts, which depend on the boundary considered and the experimental conditions, have been reported.[2,4,15] In this work, the details of the SEM-REBIC contrast or its variation as a function of the experimental parameters have not been investigated.

Scanning tunneling spectroscopy measurements have been performed in areas, grain interior, and grain boundaries, which show different recombination properties as revealed by SEM-REBIC. Figure 2 shows the $(dI/dV)/(I/V)$ curve recorded in a region far from the grain boundaries. A band gap of 3 eV, close to the bulk value of 3.2 eV, and the asymmetry related to the *n*-type nature of the sample, is observed. CITS images reveal electronic inhomogeneities at a nanoscale level, which are more readily detected near grain boundaries. Figure 3 shows a constant-current and three selected CITS images recorded at a region containing several grain boundaries, in which contrast due to local conductance variations is observed. Figure 4 shows the normalized differential conductance curves corresponding to sites marked as 1 and 2 in Fig. 3. A surface band gap of about 2.8 eV can be estimated from the curve recorded at position 1 [Fig. 4(a)], while the $(dI/dV)/(I/V)$ curve recorded at position 2, corresponding to a grain boundary, reveals a marked metallic behavior [Fig. 4(b)]. As summarized in Figs. 2 and 4, the general result of a surface band gap close to the bulk value in the grains and a reduced gap at the boundaries has been found to be reproducible in different grains and grain boundaries of the samples. The measurements were performed with different tips and under different tunneling conditions, which lead us to conclude that the curves were representative of the material investigated although they were recorded in high vacuum. This shows that the inhomogeneity revealed in the SEM-REBIC images is also apparent in the conductance curves through local surface band gap variations. The use of our combined SEM-STM system allowed a correlative study by REBIC and CITS of the same grains. Rohrer and

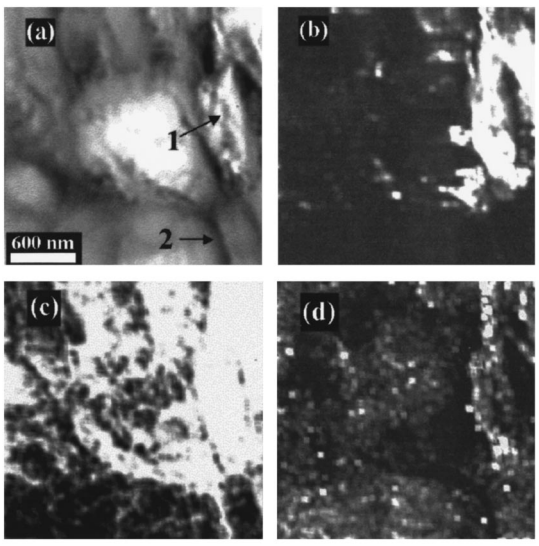

FIG. 3. STM images of a ZnO sample. (a) Topography image acquired with +1.5 V sample bias voltage and 0.44 nA tunnel current. Gray scale range is 99 nm. (b)–(d) Corresponding CITS images acquired at (b) −0.72 V, (c) −2.70 V, and (d) +2.70 V sample voltages.

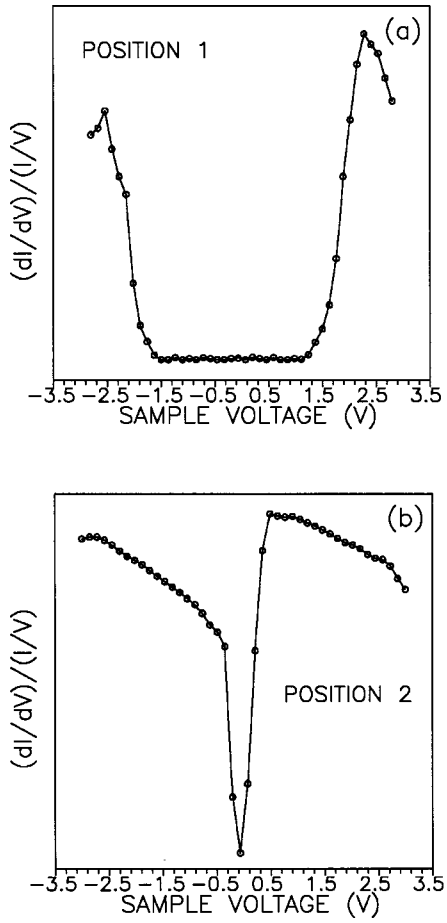

FIG. 4. $(dI/dV)/(I/V)$ dependence on applied bias voltages recorded at positions labeled (a) ''1'' and (b) ''2'' in Fig. 3.

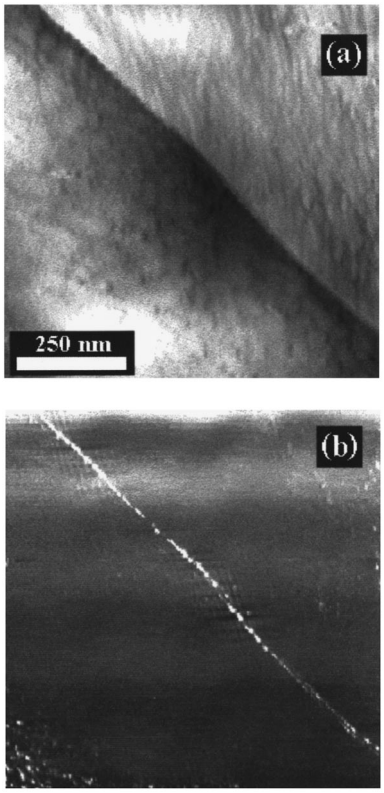

FIG. 5. (a) STM topography image of a grain boundary acquired with a sample voltage of 6 V and 4 nA tunneling current. Gray scale is 49 nm. (b) Corresponding STM-REBIC image. Gray scale range is 0.09 nA.

Bonnell[16] used spatially resolved tunneling spectroscopy to study ZnO boundaries, and concluded that areas of reduced conductivity at both sides of the boundaries were due to associated space charge regions. They measured apparent band gaps of 2 and 0.7 eV at the boundary and far away from the boundary respectively, but considered that the width of the zero conductivity region was essentially determined by instrumental parameters. The results of this work agree with those of Ref. 17 in the sense that conductance variations are detected near the grain boundaries, but in our case the band gap outside the boundary is significantly close to the ZnO bulk band gap of 3.2 eV. These differences can be explained taking into account the different nature of the samples investigated in both cases. Rohrer and Bonnell performed their STM measurements in varistor ZnO doped with Bi_2O_3 and smaller amounts of CoO, MnO, and Al, whereas undoped ZnO was used in the present work. Bi_2O_3 is not soluble in ZnO and is known to segregate to the grain boundaries. It is thought[18] that the bismuth segregation creates a negatively charged layer in the grain boundary, which induces upwards surface band bending in the adjacent ZnO crystals. The bending creates a depletion layer and increases the interfacial resistance due to the decreased carrier concentration, which in turn leads to lower tunnel currents.

The presence of space charge regions at the boundaries is also detected in STM-REBIC images. Figures 5 and 6 show the constant current and the simultaneously acquired STM-REBIC images of different grain boundaries. The size of the features resolved in the first image is about 20 nm, while a resolution of 50 nm is attained in the latter. STM-REBIC images were recorded with positive sample voltages, and contrast was observed with biases as low as 1.5 V (Fig. 6). The signal level and the quality of the STM-REBIC image increased with bias voltage up to a maximum value of 6 V. It was found that tunnel voltages higher than about 7 V caused instabilities in the tunnel current, which in turn led to fluctuations in the induced current. A comparison of the SEM-REBIC and STM-REBIC contrast of the boundaries shows marked differences. In the former case a black-white region extending several microns at both sides of the boundary was observed, as in Fig. 1. This contrast, known as peak and trough (PAT), is due to the opposite directions of the electric field on different sides of the defect,[3,5] and can be modeled as two Schottky barriers back-to-back. The PAT contrast clearly differs from the narrow, bright line contrast associated with the grain boundary shown in Fig. 5(b), but has a certain resemblance to that shown by the lower grain boundary which appears with bright and dark areas in Fig. 6(b). The latter figure also indicates that not all the boundaries imaged in the constant current mode [Fig. 6(a)] show electrical activity under the same tunneling conditions, as revealed by the lack of contrast related to the upper grain boundary observed in the corresponding STM-REBIC image [Fig. 6(b)]. All of these differences are explained by the dependence of the REBIC contrast on experimental conditions.

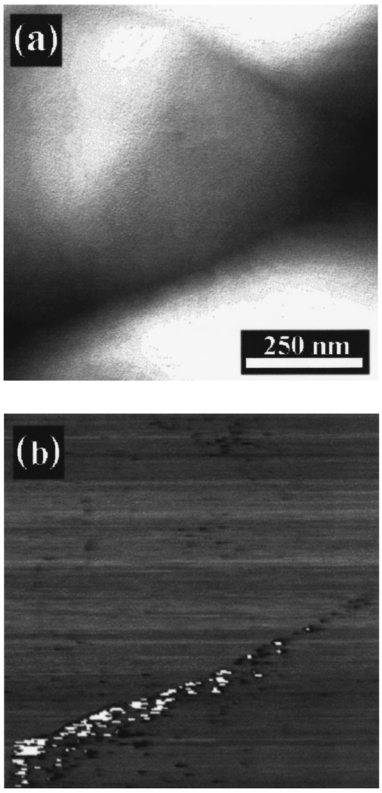

FIG. 6. (a) Constant current topography image of a ZnO surface, showing two grain boundaries, recorded with 1.2 V sample voltage and 0.32 nA tunneling current; gray scale range is 240 nm. (b) Simultaneously acquired STM-REBIC image (gray scale range is 0.12 nA).

In particular, grain boundaries and surface steps have been reported to show not only a black-white SEM-REBIC contrast but also an only black or an only white contrast depending on temperature, excitation conditions, applied bias voltage, and the nature of the defect.[2,4,5,17,19] SEM-REBIC and STM-REBIC observations of a given grain boundary correspond to completely different excitation conditions involving different parameters as carrier generation rate, sample heating and, specially, signal generation volume. The SEM electron beam range is higher than 1 μm while for an applied voltage of 10 V, of the order of magnitude of the STM bias, the dimension of the generation volume is about 5 nm.[7] The observed STM-REBIC contrast corresponds therefore to the presence of charged regions in the surface. More detailed contrast studies would be necessary, as those available for the SEM case, for a detailed interpretation of the images in terms of electric fields at the defects. The resolution of our STM-REBIC images is similar to that reported in Ref. 7 for the grain boundaries of $CuInSe_2$.

IV. CONCLUSIONS

A SEM-STM combined instrument enabled the correlative study of ZnO by SEM and STM beam-induced current techniques and by CITS. In particular, grain boundaries showing electrical activity, as detected in SEM-REBIC images, have been found by CITS to have a reduced surface band gap relative to the grain interior. Grain boundaries were imaged by STM-REBIC with a resolution of about 20 nm. REBIC contrasts in SEM and STM images are not comparable due to the different excitation conditions and signal generation volume of each technique.

ACKNOWLEDGMENT

This work was supported by DGES through Project PB96-0639.

[1] R. Einzinger, Appl. Surf. Sci. **1**, 329 (1978).
[2] A. Bernds, K. Löhnert, and E. Kubalek, J. Phys. (Paris), Colloq. **6**, 181 (1984).
[3] D. B. Holt, in *Polycrystalline Semiconductors III—Physics and Technology, Solid State Phenomena*, edited by H. P. Strunk, J. H. Werner, B. Fortin, and O. Bonnaud (Trans Tech., Zurich, 1994), Vol. 37-38, p. 171.
[4] J. D. Russell, D. C. Halls, and C. Leach, Acta Mater. **44**, 2431 (1996).
[5] D. B. Holt, B. Raza, and A. Wojcik, Mater. Sci. Eng., B **42**, 14 (1996).
[6] A. Gustafsson, M. Pistol, L. Montelius, and L. Samuelson, J. Appl. Phys. **84**, 1715 (1998).
[7] L. L. Kazmerski, J. Vac. Sci. Technol. B **9**, 1549 (1991).
[8] P. Koschinski, V. Dworak, P. E. West, and L. J. Balk, Scanning Microsc. **10**, 33 (1996).
[9] A. Asenjo, A. Buendía, J. M. Gómez-Rodríguez, and A. Baró, J. Vac. Sci. Technol. B **12**, 1658 (1994).
[10] R. M. Feenstra, Surf. Sci. **299-300**, 965 (1994).
[11] R. J. Hamers, R. M. Tromp, and J. E. Demuth, Phys. Rev. Lett. **56**, 1972 (1986).
[12] J. A. Stroscio, R. M. Feenstra, and A. P. Fein, Phys. Rev. Lett. **57**, 2579 (1986).
[13] N. D. Lang, Phys. Rev. B **34**, 5947 (1986).
[14] R. M. Feenstra, J. A. Stroscio, and A. P. Fein, Surf. Sci. **181**, 295 (1987).
[15] J. T. C. van Kemenade and R. K. Eijnhoven, J. Appl. Phys. **50**, 2431 (1979).
[16] G. S. Rohrer and D. A. Bonnell, J. Am. Ceram. Soc. **73**, 3026 (1990).
[17] G. Panin and E. Yakimov, Semicond. Sci. Technol. **7**, 150 (1992).
[18] W. G. Morris, J. Vac. Sci. Technol. **13**, 926 (1976).
[19] C. Díaz-Guerra and J. Piqueras, Appl. Phys. Lett. **71**, 2830 (1997).